Vehicle dynamics model for simulation on a microcomputer

R.M. Brach

Aerospace & Mechanical Engineering, University of Notre Dame, Notre Dame, Indiana, USA

Abstract: Equations of motion are derived for a two-axle, two-wheeled vehicle pulling a one-axle, two-wheeled trailer. Linear and nonlinear tyre side force models are discussed. Examples of computer solutions of the equations are presented for both single vehicle motion and articulated vehicle motion. A comparison of tractor semitrailer manoeuvres with a more elaborate simulation shows excellent results.

Reference to this article should be made as follows: Brach, R.M. (1991) 'Vehicle dynamics model for simulation on a microcomputer', *Int. J. of Vehicle Design*, vol. 12, no. 4, pp. 404–419.

Keywords: articulated vehicles, equations of motion, microcomputer, simulation, single vehicles, vehicle dynamics.

1 Introduction

The vehicle dynamical simulation described here is intended to produce a general purpose simulation of moderate complexity. The availability of microcomputers permits calculations of the type discussed here to be made in almost a routine fashion. As a result, more and more engineering facilities are capable of these types of calculations. Along with model development, this article is also intended to provide a range of sample solutions to which other simulations can be compared.

Different approaches to vehicle dynamics problems are briefly discussed to provide a perspective. At least four different approaches typically are used to solve vehicle dynamics problems:

1 Analytical solutions for stability analysis.
2 Special purpose simulation models.
3 Comprehensive computerized solutions of multidegree of freedom models for general simulation.
4 Application of general purpose, mechanical engineering multibody simulation software packages.

The first type of analyses begins with a simplified physical model with up to 3 or 4 degrees of freedom and is followed by a steady forward speed or steady turn constraint. The resulting equations are then solved in a manner which indicates the effect of various parameters on the steady motion. (For example, see Ellis, 1969, Huston and Johnson, 1983, Passarello, 1979 and Klein and Szostak, 1980). These methods have been extremely important in providing basic stability information for vehicle systems. They do not explicitly provide the motion of the vehicles. The second type of models provide specialized motion simulations, such as the collision of vehicles with other vehicles or barriers covered by McHenry and McHenry, 1988a and 1988b, along with post-impact motion.

The simulation model presented fits into the third category. This consists typically of the solution of the differential equations of motion of a single vehicle or articulated vehicle system. These models can range widely in complexity. For example, an existing single vehicle simulation of Allen *et al.*, 1988 includes the effects of steering, driver response, nonlinear tyre mechanics, a flexible suspension system, etc. For trucks, a comprehensive simulation has been developed by HSRI/MVMA; see Gillespie, 1978 and Hayes, 1980. A comprehensive set of experiments was conducted colaterally in Phase 4 of that model's development. Phase 4 simulation results are used for comparison with the results of the simulation.

The last category of simulations is of relatively recent origin. Numerous general purpose dynamical computer simulation programs have been developed which apply to a broad variety of machines. They are commercially available as software packages. Some have been applied to automotive vehicles, both on road and off road as in Croscheck and Ford, 1988, Molnar, and Claar and Zie, 1988. The last reference provides a review of the available packages; it also provides an excellent review of various methods available for deriving dynamical equations of motion.

Obviously, the more comprehensive the physical model being simulated and the more attention paid to modelling vehicle components (tyre elasticity and damping, transverse suspension flexibility, wheel-brake slip drag, etc.), the wider the applicability and the greater the potential for accurate predictions. Unfortunately, this capability comes with a price, namely, a greater amount of input information is required in order to use the simulation effectively. Often, this information is unavailable. Another factor which often lessens the need for high accuracy is the variability of behaviour across 'identical' vehicles. Vehicle-to-vehicle variations can be significant but are seldom measured (because of cost). Even significant left-to-right asymmetries in the same vehicle can sometimes occur as noted by Gillespie, 1978. Consequently, the capability of highly accurate prediction techniques in some applications may be unnecessary. For this reason, the simulation model has the objective of being a general purpose one of moderate complexity, sufficient to take into account most of the important vehicle physical factors.

The simulation developed includes a tow vehicle pulling a trailer over a flat surface (two-dimensional motion). By proper formation of a solution algorithm, the mass of the trailer can be set to zero, yielding single vehicle simulation. A computer solution is not provided, but the equations of motion are derived and listed in an Appendix. The equations are for the dual-vehicle kinematics and geometry only; external forces are included in the equations but, with two exceptions, they are not modelled. For example, the equations of aerodynamic forces are not presented. The two exceptions are tyre force models. Equations for sliding friction and a nonlinear steering force model are provided.

Examples of computerized solutions are presented to illustrate the versatility of the model and to compare its results to some Phase 4 simulation results.

2 Equations of motion

The coordinate system, assumptions and equations of motion are discussed in this section. The final set of differential equations and an explanation of notation are provided in Appendix A; their derivation is summarized here. The coordinate system used is an inertial system fixed to the flat level plane surface. The vehicle system consists of a two vehicle, C (car or cab) and a trailer T, as shown in Figure 1. In the remainder of this article, the

Figure 1 Diagram of the tow vehicle and trailer showing tyre force components, vehicle, dimensions, distances and the coordinate system

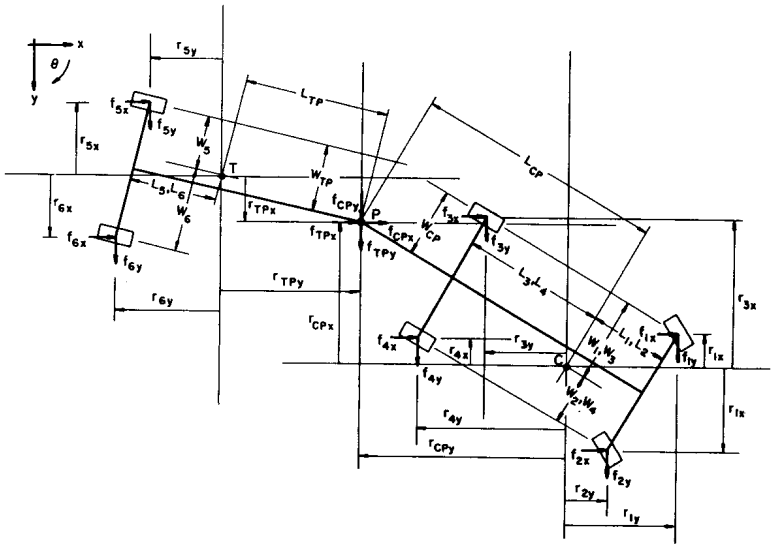

tow vehicle will be referred to as the car (or in some applications as a tractor). Direct applications of Newton's second law in component form provides six equations as follows:

$$m_c \ddot{x}_c = f_{cpx} + \sum_{i=1}^{4} f_{ix} + F_{cx} \tag{1}$$

$$m_c \ddot{y}_c = f_{cpy} + \sum_{i=1}^{4} f_{iy} + F_{cy} \tag{2}$$

$$J_c \ddot{\theta}_c = r_{cpy} f_{cpy} + r_{cpx} f_{cpx} + \sum_{i=1}^{4} (r_{ix} f_{ix} + r_{iy} f_{iy}) + M_c \tag{3}$$

$$m_t \ddot{x}_t = f_{tpx} + \sum_{i=5}^{6} f_{ix} + F_{tx} \tag{4}$$

$$m_t \ddot{y}_t = f_{tpy} + \sum_{i=5}^{6} f_{iy} + F_{ty} \tag{5}$$

$$J_t \ddot{\theta}_t = r_{tpy} f_{tpy} + r_{tpx} f_{tpx} + \sum_{i=5}^{6} (r_{ix} f_{ix} + r_{iy} f_{iy}) + M_t. \tag{6}$$

The connection of the trailer and car at the pin, P, provides two constraint equations which must be taken into account. The position components of the trailer mass centre can be expressed in terms of the mass centre positions of the car as:

$$x_t = x_c - R_{cp} \sin\theta_{cp} - R_{tp} \sin\theta_{tp} \tag{7}$$

$$y_t = y_c - R_{cp} \cos\theta_{cp} - R_{tp} \cos\theta_{tp}. \tag{8}$$

Equations 1 to 6 represent a system with six degrees of freedom. The car trailer system has only four degrees of freedom. Equations 7 and 8 are used to reduce equation 6 to a set of four independent equations. The velocity and acceleration components $\dot{x}_t$, $\dot{y}_t$, $\ddot{x}_t$ and $\ddot{y}_t$ are also needed and can be obtained by direct differentiation of equations 7 and 8.

By Newton's third law, the pin force components f_{cpx} and f_{cpy} on the car must be equal and opposite to the pin forces f_{tpx} and f_{tpy}, respectively, on the trailer. Addition of equations 1 and 4 and equations 2 and 5 causes them to cancel. After adding these equations, the acceleration $\ddot{x}_t$ is eliminated by using the second derivative of equation 7 and $\ddot{y}_t$ is eliminated by using the second derivative of equation 8. Equations A1 and A2 in the Appendix result from this procedure and are the first two of the final four system equations.

Equations 3 and 6 provide two more equations of motion but the pin force components again must be eliminated. This can be done in the following way. Equation 1 is solved for f_{cpx} and equation A1 is used to eliminate $\ddot{x}_c$. Then f_{cpy} is obtained from equation 2 with $\ddot{y}_c$ eliminated using equation A2. These expressions for f_{cpx} and f_{cpy} are then substituted into equation 3, which is then solved for $\ddot{\theta}_c$ and listed in Appendix A as equation A3. Similarly, f_{ctx} and f_{cty} (which are equal and opposite in sign to f_{cpx} and f_{cpy}) are eliminated from equation 6. Solution of this equation for $\ddot{\theta}_t$ results in equation A4.

Equations A1, A2, A3 and A4 provide a set of four second order differential equations for the car–trailer system. If a single vehicle simulation is desired, m_t is set to zero and only the first three equations are integrated. Careful examination shows that they are not uncoupled in the acceleration terms, as desired for integration. At least two approaches are possible. Though coupled, equations A1 to A4 are linear and algebraic in the acceleration terms. Each acceleration can be determined numerically using a linear equation routine at each time step of the integration. An alternative is to simply use the immediate past values for the angular acceleration terms still remaining on the right-hand sides of equations A1 to A4. Both approaches yield good results; the latter approach is used for the results presented.

3 Single vehicle dynamics

If the trailer mass is set to zero and only the first three equations of motion are integrated, the model provides the dynamics of a single vehicle. Before the equations can be integrated, the force system at the tyre ground interface must be specified. Some typical tyre models are discussed briefly with examples provided to illustrate their utility.

3.1 Locked wheel skidding

One of the simplest tyre force models is Coulomb friction. A reasonably general model consists of a friction force which varies linearly with speed. It is known that sliding frictional forces are lower at high speeds than at lower speeds; see Reed and Keskin, 1987 and Brach, 1972. This is particularly evident on wet pavements. An appropriate model for a generalized friction coefficient is:

$$\mu = \mu_o - kv \tag{9}$$

where μ_o is the low speed sliding coefficient, v is the wheel velocity and k is a rate at which the friction decreases with speed. Other, nonlinear, models can also be developed as in Allen *et al.*, 1988. The vertical force, F_z, at each wheel is multiplied by μ to give the frictional force which directly opposes each wheel's velocity. It is relatively easy to program changes of μ_o and k in equation 9 to vary over the ground surface coordinates x and y in order to simulate frictional variations such as patches of ice, local surface contamination, etc. Each wheel's sliding force is determined independently.

A subtle, but important, point must be mentioned relative to a Coulomb friction model such as equation 9. Near the end of a skid, when some or all of the wheels' speeds are near zero, the above model is unstable during numerical integration. Sign changes in a wheel's velocity can occur at speeds near zero causing a frictional force which 'speeds up' the vehicle; this is referred to in Allen *et al.*, 1988. This can be avoided by requiring the coefficient to smoothly approach zero below some small speed, say 0.5 m/sec.

Table 3 lists the physical parameters of an automobile and some other vehicles. Table 1 lists the results of three locked wheel skid simulations for the automobile from an initial speed of 22.35 m/s (50 mph). This was done with the right wheels on a lower coefficient surface than the left such as encountered on partially icy pavements or when one wheel is off of the paved portion of a road. One case includes the effects of load transfer due to a mass centre height of 0.5 m (see later). It is interesting to note that the coefficient split from 0.75/0.55 to 0.75/0.35 causes an increase in stopping distance of about 20% but an increase of over 200% in angular rotation. Figure 2 illustrates these results.

3.2 *Modelling for steering control and vertical load transfer*

The simplest tyre force model which gives good results in many applications is the linear model,

$$F_t = C_\alpha \alpha \tag{10}$$

Table 1 Single vehicle motion, initial speed 22.4 m/s (50 mph) locked wheel skid, dual coefficient pavement

Time, sec	μ = .75/.35 x_c meters	$h_c = 0$ θ_c deg	μ = .75/.55 x_c meters	$h_c = 0$ θ_c deg	μ = .75/.55 x_c meters	h_c = 0.5 m θ_c deg
0.00	0.00	0.00	0.00	0.00	0.00	0.00
0.60	12.44	–7.29	12.26	–3.61	12.26	–3.64
1.20	22.94	–27.40	22.23	–13.46	22.25	–13.66
1.80	31.53	–59.22	29.91	–27.73	29.97	–28.51
2.40	38.12	–109.50	35.33	–45.06	35.46	–47.02
3.00	42.75	–173.35	38.44	–65.88	38.57	–69.86
3.60	45.59	–224.02	39.34	–83.26	39.48	–89.19
4.20	46.82	–257.73				
4.56	47.04	–264.64				

Table 2 Steer angle magnitudes for the 3.7 m, 3-sec lane change of Figure 5

Vehicle Speed	Magnitude of Steer Angle, deg: Linear Tire Model	Nonlinear Model
13.4 m/s (30 mph)	3.050	3.050
22.4 m/s (50 mph)	1.260	1.260
31.3 m/s (70 mph)	0.775	0.770
40.2 m/s (90 mph)	0.570	0.560

Table 3 Vehicle parameters or example simulations

AUTOMOBILE:

m_c = 1496 kg	J_c = 3004 kg–m^2
L_1=L_2 = 1.25 m	L_3=L_4 = 1.55 m
W_1=W_2 = 0.76 m	W_3=W_4 = 0.76 m
W_{cp} = 0.76 m	L_{cp} = 2.83 m
h_c = 0.52 m	$C_{\alpha 1}$=$C_{\alpha 2}$ = 506 N/deg
$C_{\alpha 3}$=$C_{\alpha 4}$ = 456 N/deg (without trailer)	
$C_{\alpha 3}$=$C_{\alpha 4}$ = 1118 N/deg (with trailer)	

AUTOMOBILE TRAILER:

m_t = 2160 kg	J_t = 7759 kg–m^2
L_5=L_6 = 0.43 m	W_5=W_6 = 1.10 m
W_{tp} = 1.10 m	L_{tp} = 3.87 m
h_t = 0.76 m	$C_{\alpha 5}$=$C_{\alpha 6}$ = 1281 N/deg

TRUCK TRACTOR:

m_c = 7891 kg	J_c = 43493 kg–m^2
L_1=L_2 = 1.74 m	L_3=L_4 = 2.07 m
W_1=W_2 = 1.01 m	W_3=W_4 = 1.01 m
W_{cp} = 1.01 m	L_{cp} = 2.07 m
h_c = 0.61 m	
$C_{\alpha 1}$=$C_{\alpha 2}$ = 2236 N/de	$C_{\alpha 3}$=$C_{\alpha 4}$ = 7701 N/deg

TRUCK SEMITRAILER:

m_t = 23354 kg	J_c = 159583 kg–m^2
L_5=L_6 = 4.28 m	W_5=W_6 = 0.91 m
W_{tp} = 0.91 m	L_{tp} = 5.45 m
h_t = 0.76 m	$C_{\alpha 5}$=$C_{\alpha 6}$ = 7453 N/deg

where F_t is the force component transverse to the tyre heading, C_α is a constant called the tyre side force coefficient and α is the side slip angle of the wheel. The side slip angle is the angle between the wheel's heading and its velocity vector. Many publications exist on the subject of nonlinear modelling of tyre mechanics. Two of them are Bakker *et al.*, 1987 and Bergman, 1977. Both contain equations which can be programmed to provide tyre forces and moments which agree quite well with experimental results, yet which are

Figure 2 Locked wheel skid over a dual coefficient of friction surface; initial speed is 22.4 m/sec (50 mph). Left/right coefficients are 0.75/0.55 for the top figure and 0.75/0.35 for the bottom

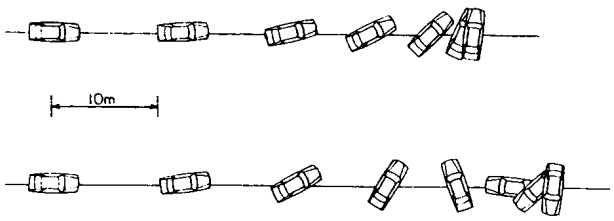

Figure 3 Nonlinear tyre force model (Bakker *et al.*, 1987); each curve has the same coefficient, C_α, but saturates at levels dependent upon the normal force, F_z

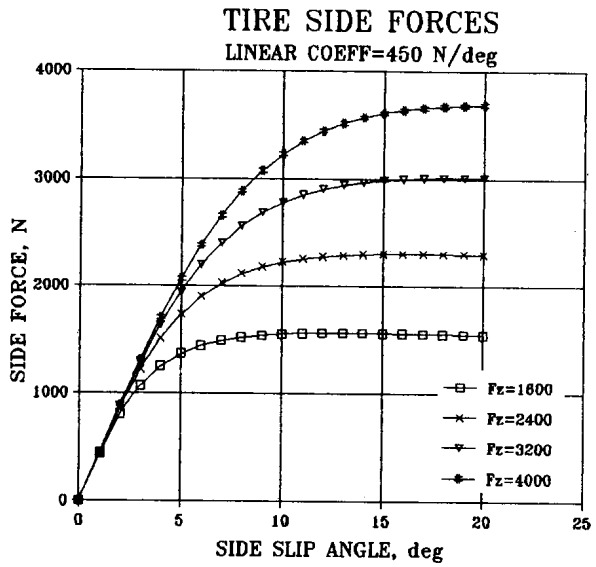

not unduly complicated. The following set of equations is a simplification of the model presented by Bakker, Nyborg and Pacejka, 1987:

$$A = (-0.0221\,F_z + 1.011)F_z \qquad B = -0.354\,F_z + 0.707$$
$$D = C_\alpha/(1.30\,A) \qquad E = (1-B)\alpha + (B/D)\,\mathrm{atn}\,(\alpha D)$$
$$F_t = A\sin(1.30\tan^{-1}|D\,E|) \qquad (11)$$

F_z is the normal force in Newtons, C_α is the initial slope of the tyre side force in units of N/deg and α is the side slip angle in degrees. Refer to Bakker *et al.*, 1987 for the form and source of the constants. The characteristics of this model are shown in Figure 3. In

Figure 4 Example of a steering angle which simulates a lane change or avoidance manoeuvre; it is composed of offset sine functions

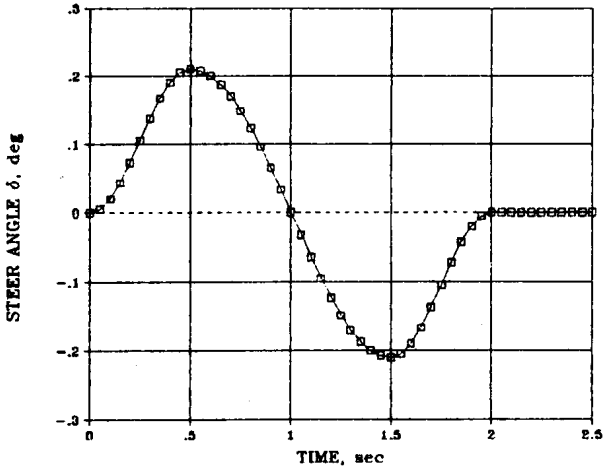

the remainder of this paper, the tyre model given by equation 11 is referred to as the nonlinear tyre model.

Equation 11 for the tyre side force contains the effect of varying normal force F_z. The equations of motion derived earlier do not contain the effects of a flexible suspension system. Consequently, the normal forces take on only their static values. It is possible to approximate dynamic load transfer by using lateral and fore-and-aft moments created by the respective acceleration components acting through the vehicles' centres of gravity at heights h_c and h_t. (The equations are relatively simple and are not presented here.) This causes F_z to vary about the static value for each wheel during turning, accelerating and braking. Through equation 11, this causes the lateral tyre forces to vary dynamically between the load curves illustrated in Figure 3.

Dynamic normal force variations from wheel to wheel can also affect locked wheel skidding when the friction coefficient is not constant over the ground surface. Table 1 illustrates this effect; it is small but not insignificant. No experimental data appear to be available for comparisons with the model results.

A lane change manoeuvre is used to illustrate the tyre force model (equation 11) and the load transfer approximation for a vehicle under steering control. Figure 4 shows a convenient representation of a front wheel steer angle composed of offset segments of sine functions. It will produce a lateral position change for a forward moving vehicle. Table 2 shows the magnitude of the steer angle of Figure 4 for the car in Table 3, for a lane change at four forward speeds. In all cases, a lateral position change of 3.66 m (12 ft) takes place in 3 seconds. Note that the linear and nonlinear tyre models (and corresponding absence and inclusion of load transfer) produced identical results. This implies that the nonlinear effects and load transfer are not significant for this specific example. The vehicle's yaw velocity is plotted in Figure 5 for the four speeds simulated.

Figure 5 Yaw angular velocity for an automobile undergoing a lane change at four different speeds for the steer angle of Figure 4

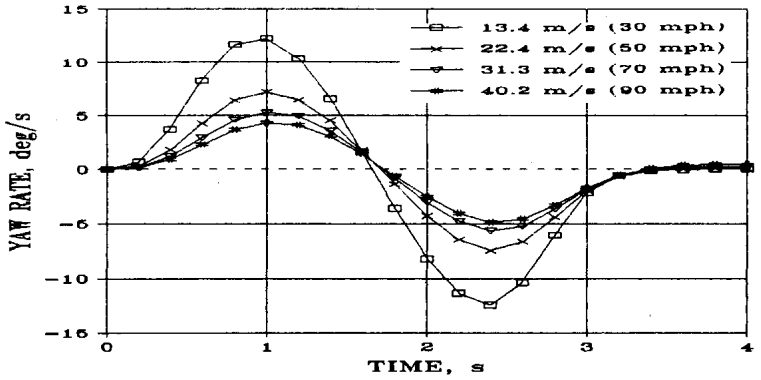

4 Articulated vehicle dynamics

The full model composed of a tow vehicle (car or cab) and trailer will be discussed and illustrated in this section. Two sample cases are presented. The first is that of a car pulling a recreational trailer and is used to illustrate that motion can be unstable at high speeds. The second is a simulation of a tractor semi-trailer and a comparison of the simulation with the Phase 4 simulation.

4.1 Car/trailer stability

At sufficiently high speeds, the lateral motion of a car and trailer can become unstable. A single, sample configuration of a car and recreational trailer is used to illustrate the instability and how different tyre model combinations affect the motion. It is assumed that a load equalizing hitch is used such that the static, vertical front wheel loads are the same as the car of Table 3 without the trailer. The car's rear wheel static vertical loads increase due to the trailer; in addition the rear tyre side force coefficient is increased significantly.*

For this example, the car and trailer initially are moving straight ahead at 26.8 m/s (60 mph) and then at 54.6 m/s (120 mph). A steer angle with a maximum of 0.21 degrees over a two-second interval as illustrated in Figure 4 is given to the car's front wheels. Figure 6 shows the yaw velocity of the trailer and Figure 7 shows the relative yaw angle between the car and trailer. At the lower speed, the vehicle motions are stable and virtually identical for both linear and nonlinear tyre models. At the higher speed, the motion is unstable because the yaw motion diverges after the steering manoeuvre is completed. Differences in the motion for the different tyre models do occur; they appear to become significant for relative yaw angles greater than about 5 degrees.

Examination of Figure 3 shows that the nonlinear tyre model has a characteristic limiting value to the side force whereas the side force in the linear model continues to increase with side slip angle. Large side forces can exceed the frictional limits between the tyre and pavement and lead to sliding. This happened to the trailer wheels with the linear tyre model (for a friction coefficient of 1.0) and is evident in Figure 6 near t=9.5 sec.

*The physical characteristics of the car and recreational trailer simulated are not intentionally representative of any specific vehicles.

Figure 6 Trailer yaw velocity for an automobile trailer combination undergoing a two-second avoidance manoeuvre:
A nonlinear tyre model, load transfer included
B nonlinear tyre model, no load transfer (h=0)
C linear tyre model, no load transfer
D nonlinear tyre model, no load transfer

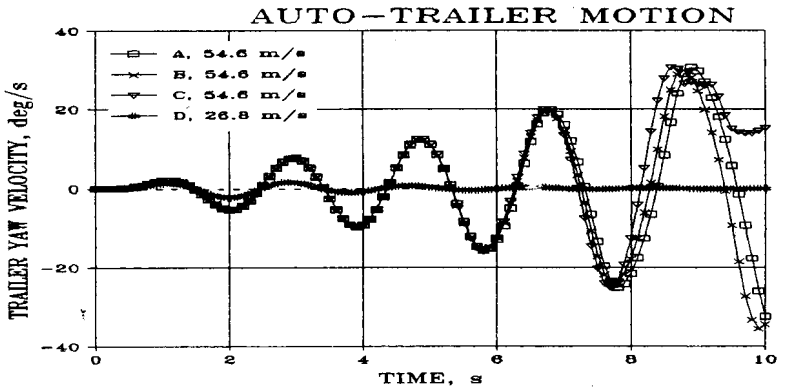

Figure 7 Relative angle between the automobile and trailer for a two-second avoidance manoeuvre:
A nonlinear tyre model, load transfer included
B nonlinear tyre model, no load transfer (h=0)
C linear tyre model, no load transfer
D nonlinear tyre model, no load transfer

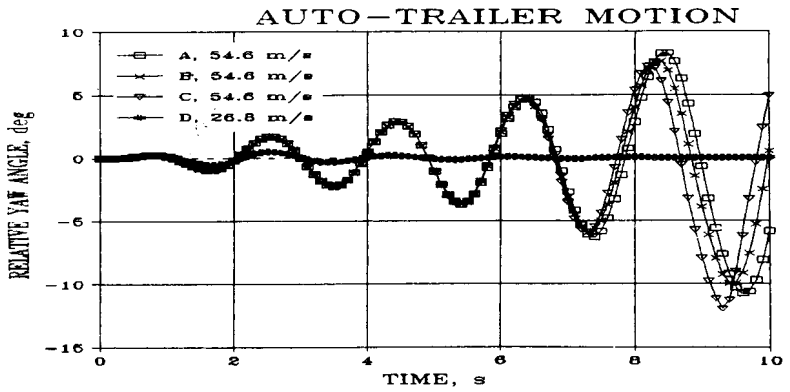

4.2 *Tractor semi-trailer, simulation comparison*

Several manoeuvres and loading condition combinations were simulated with the Phase 4 computer program as part of a comprehensive truck modelling research program; refer to Hayes, 1980. One combination is used here for comparison of the equations. The front wheel steering angle corresponding to a lane change manoeuvre is illustrated in Figure 8. The digitized values of steer angle were interpolated quadratically for use in the simulation. The pertinent vehicle data is taken from Hayes, 1980 and is listed in Table 3. For this particular test, the tractor semitrailer was in a loaded condition manoeuvring over a flat high friction surface.

Four aspects of the vehicles' response are compared in Figures 9 to 12. In each case, the results are shown for the linear tyre model (LTM) and nonlinear tyre model (NLTM). The response using the linear tyre model matches very closely while the nonlinear tyre model does not do as well. No attempt was made to adjust any of the NLTM parameters to bring it into closer agreement.

One adjustment was made to the vehicles' physical parameters in this simulation. Since the simulation uses a rigid suspension system with a simple inertial load transfer, the heights of the mass centres had to be modified. It was decided to use a percentage of the mass centre height of the tractor's and semitrailer's sprung masses. With full heights used for h_c and h_t, the vertical tyre forces for the tractor wheels were close to the Phase 4 values but the computer results showed the right rear trailer wheel raising from the road surface (negative force) near the 4 to 5 sec time interval (see Figure 12). Values of 60% of the tractor's sprung mass height for h_c and 40% of the trailer's for h_t gave the results shown in the Figures.

In general, the results of both simulations match quite well, perhaps surprisingly well considering the simplicity of the model and the severity of the manoeuvre. At a speed

Figure 8 Experimentally measured front wheel steering angle (Hayes, 1980)

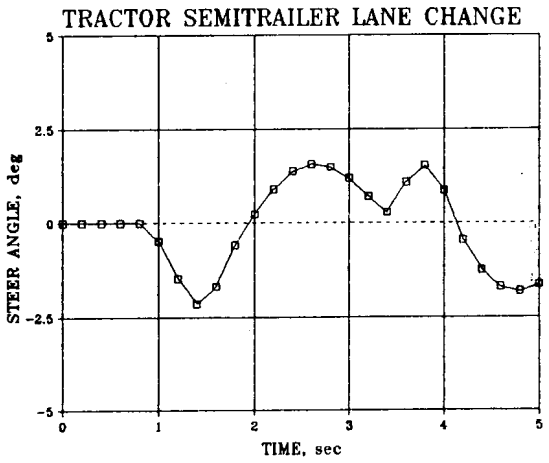

Figure 9 Comparison of the simulation model with simulation of Phase 4 of Hayes, 1980; LTM is with a linear tyre model and NLTM is for the non-linear tyre model

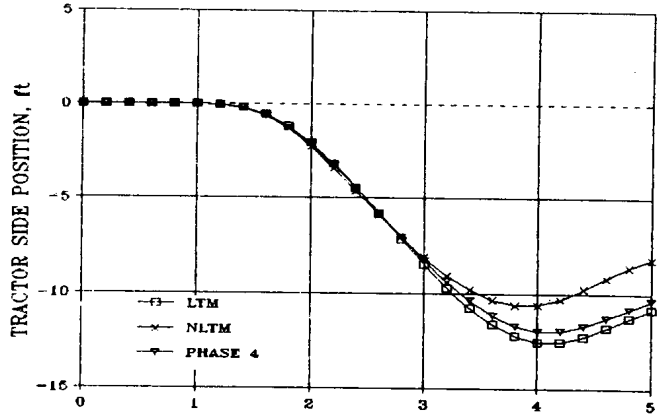

Figure 10 Comparison of the simulation model with simulation of Phase 4 of Hayes, 1980; LTM is with a linear tyre model and NLTM is for the non-linear tyre model

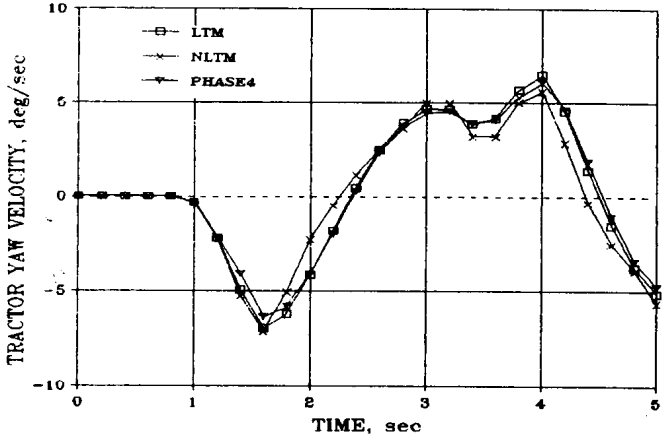

of 108 km/h (67 mph) a steering angle change of -2.27 deg to $+1.57$ degrees in an interval of about 1 second is very severe for a vehicle of this type and weight.

5 Computer hardware and software

The simulation results were from a computer program written in the Microsoft QuickBASIC compiled language. Separate subroutines were written to handle the following:

Figure 11 Comparison of the simulation model with simulation of Phase 4 of Hayes, 1980; LTM is with a linear tyre model and NLTM is for the non-linear tyre model

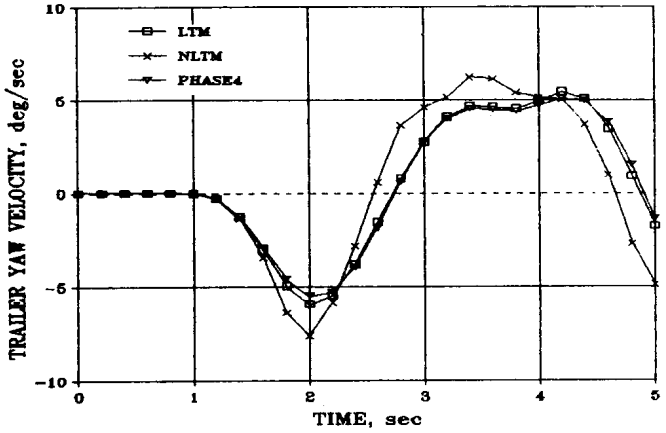

Figure 12 Comparison of the simulation model with simulation of Phase 4 of Hayes, 1980; LTM is with a linear tyre model and NLTM is with the non-linear tyre model. Simulated centre of gravity heights are at 60% and 40% of sprung mass heights of tractor and semitrailer, respectively.

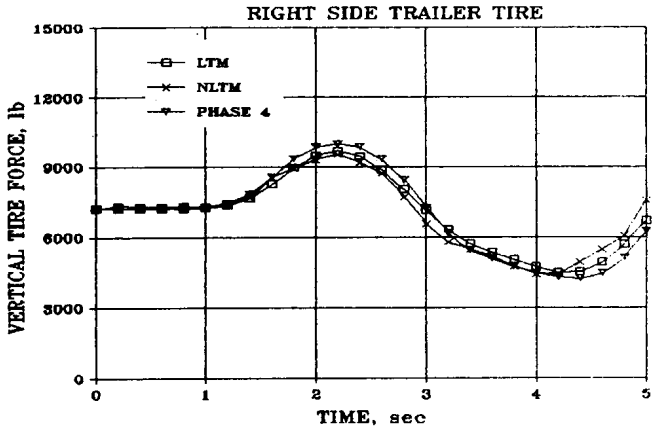

1 Tyre–ground force calculation, including steering or locked wheel skidding.
2 Static, vertical wheel load calculation; hitch load equalization when necessary.
3 Inertial load transfer, side to side and fore to aft.
4 Numerical integration of the differential equations.
5 Output to monitor, printer and/or diskette file.
6 Quadratic interpolation for tabular steering inputs.

The numerical integration technique used is the well known fourth-order Runge-Kutta-Gill method. The computer uses the MS/DOS operating system. It has a processor speed of 25 MHz and used a numeric coprocessor chip. This computer and language combination provides a compilation time of about 10 seconds and a run time (tractor semitrailer simulation) of about 60 seconds. All calculations were single precision; the integration interval was 0.01 sec.

Appendix A Notation and equations of motion

The four differential equations of motion for a tow vehicle pulling a trailer are contained in this Appendix. Equations defining intermediate variables are presented along with a list of symbols. All of the variables are illustrated in Figure 1. The equations of motion are:

$$(m_c + m_t)\,\ddot{x}_c = -m_t\left(R_{cp}\,\ddot{\theta}_{cp}\cos\theta_{cp} + R_{cp}\,\dot{\theta}_{cp}^2\sin\theta_{cp} + R_{tp}\,\ddot{\theta}_t\cos\theta_{tp} + R_{tp}\,\dot{\theta}_t^2\sin\theta_{tp}\right) + \sum_{i=1}^{6} f_{ix} + F_{cx} + F_{tx} \tag{A1}$$

$$(m_c + m_t)\,\ddot{y}_c = -m_t\left(-R_{cp}\,\ddot{\theta}_c\sin\theta_{cp} + R_{cp}\,\dot{\theta}_c^2\cos\theta_{cp} - R_{tp}\,\ddot{\theta}_t\sin\theta_{tp} + R_{tp}\,\dot{\theta}_t^2\cos\theta_{tp}\right) + \sum_{i=1}^{6} f_{iy} + F_{cy} + F_{ty} \tag{A2}$$

$$\left[J_c + \frac{m_c m_t}{m_c + m_t}R_{cp}\left(r_{cpx}\cos\theta_{cp} - r_{cpy}\sin\theta_{cp}\right)\right]\ddot{\theta}_c = \sum_{i=1}^{4}\left(r_{ix}f_{ix} + r_{iy}f_{iy}\right) + r_{cpx}\left(\frac{m_c}{m_c + m_t}\sum_{i=1}^{6} f_{ix} - \sum_{i=1}^{4} f_{ix}\right) + r_{cpy}\left(\frac{m_c}{m_c + m_t}\sum_{i=1}^{6} f_{iy} - \sum_{i=1}^{4} f_{iy}\right) - r_{cpy}\frac{m_c m_t}{m_c + m_t}\left(R_{cp}\,\dot{\theta}_c^2\cos\theta_{cp} - R_{tp}\,\ddot{\theta}_t\sin\theta_{tp} - R_{tp}\,\dot{\theta}_t^2\cos\theta_{tp}\right) - r_{cpx}\frac{m_c m_t}{m_c + m_t}\left(R_{cp}\,\dot{\theta}_c^2\sin\theta_{cp} + R_{tp}\,\ddot{\theta}_t\cos\theta_{tp} + R_{tp}\,\dot{\theta}_t^2\sin\theta_{tp}\right) \tag{A3}$$

$$\left[J_t + \frac{m_c m_t}{m_c + m_t}R_{tp}\left(r_{tpy}\sin\theta_{tp}\right.\right.$$

$$- r_{tpx} \cos \theta_{tp}) \Big] \ddot{\theta}_t = \sum_{i=5}^{6} (r_{ix} f_{ix} + r_{iy} f_{iy})$$
$$+ r_{tpx} \left(\sum_{i=1}^{4} f_{ix} - \frac{m_c}{m_c + m_t} \sum_{i=1}^{6} f_{ix} \right)$$
$$+ r_{tpy} \left(\sum_{i=1}^{4} f_{iy} - \frac{m_c}{m_c + m_t} \sum_{i=1}^{6} f_{iy} \right)$$
$$+ r_{tpy} \frac{m_c m_t}{m_c + m_t} \left(-R_{cp} \ddot{\theta}_c \sin \theta_{cp} \right.$$
$$\left. + R_{cp} \dot{\theta}_c^2 \cos \theta_{tp} + R_{tp} \dot{\theta}_t^2 \cos \theta_{tp} \right)$$
$$+ r_{tpx} \frac{m_c m_t}{m_c + m_t} \left(R_{cp} \ddot{\theta}_c \cos \theta_{cp} \right.$$
$$\left. + R_{cp} \dot{\theta}_c^2 \sin \theta_{cp} + R_{tp} \dot{\theta}_t^2 \sin \theta_{tp} \right) \quad \text{(A4)}$$

Variables used above include:

$$R_{cp} = [L_{cp}^2 + (W_3 - W_{cp})^2]^{1/2} \quad \text{(A5)}$$

$$R_{tp} = [L_{tp}^2 + (W_{tp} - W_5)^2]^{1/2} \quad \text{(A6)}$$

$$\theta_{cp} = (\pi/2) - \theta_c - \tan^{-1} [(W_3 - W_{cp})/L_{cp}] \quad \text{(A7)}$$

$$\theta_{tp} = (\pi/2) - \theta_t - \tan^{-1} [(W_{tp} - W_5)/L_{tp}] \quad \text{(A8)}$$

$$r_{tpx} = -L_{tp} \sin \theta_t - (W_{tp} - W_5) \cos \theta_t \quad \text{(A9)}$$

$$r_{tpy} = L_{tp} \cos \theta_t - (W_{tp} - W_5) \sin \theta_t \quad \text{(A10)}$$

$$r_{cpx} = L_{cp} \sin \theta_c + (W_3 - W_{cp}) \cos \theta_c \quad \text{(A11)}$$

$$r_{cpy} = -L_{cp} \cos \theta_c + (W_3 - W_{cp}) \cos \theta_c \quad \text{(A12)}$$

NOTATION

F_{cx}, F_{cy}	External force components on car (tow vehicle)
F_{tx}, F_{ty}	External force components on trailer
F_z	Normal force between a wheel and the ground
f_{ix}, f_{iy}	Components of the tangential force between the ith tire and the ground
h_c, h_t	Heights of car and trailer centers of gravity, respectively
J_c, J_t	Mass moment of inertia of car (tow vehicle) and trailer, respectively, about their centroidal yaw axis
L_{cp}, L_{tp}	Longitudinal distance from vehicle centroidal axis to pin in each vehicle, respectively
L_i	Longitudinal distance from centroidal axes to the ith wheel
m_c, m_t	Mass of car (tow vehicle) and trailer respectively
r_{cpx}, r_{cpy}	Moment arms from tow vehicle centroidal axes to force components f_{cpx} and f_{cpy}, respectively
r_{tpx}, r_{tpy}	Moment arms from trailer centroidal axes to force components f_{tpx} and f_{tpy}, respectively
r_{ix}, r_{iy}	Moment arms from vehicle centroidal axes to tire/ground force components f_{ix} and f_{iy}, respectively
W_{cp}, W_{tp}	Transverse distance from wheel 3 and wheel 5 in each vehicle, respectively, to the pin
x, y	Ground based inertial coordinates
δ	Front wheel steer angle
i	Corresponds to a wheel number; from driver's perspective, left front (1), right front (2), left rear (3), right rear (4), left trailer (5) and right trailer (6)
c	cab or car (tow vehicle)
t	trailer

References

Allen, R.W., Rosenthal, T.J. and Szostak, H.T. (1988) *Analytical Modeling of Driver Response in Crash Avoidance Maneuvering, Vol. 1: Technical Background*, DOT HS 807 270.

Bakker, E., Nyborg, L. and Pacejka, H.B. (1987) 'Tire modelling for use in vehicle dynamic studies', SAE Technical Paper 870421.

Bergman, W. (1977) 'Critical review of the state-of-the-art in tire force and moment measurements', SAE Technical Paper 770331.

Brach, R.M. (1972) 'Friction and the mechanics of skidding automobiles', U.S. Highway Research Record No. 376, NCHRP.

Claar II, P.W. and Xie, L. (1988) 'Computer-oriented analytical dynamics for the formulation of equations of motion for complex vehicle systems', SAE Technical Paper 881310.

Croscheck, J. and Ford, M. (1988) 'Simulation takes three-wheeler for a spin', *Mechanical Engineering Magazine*, ASME.

Ellis, J.R. (1969) *Vehicle Dynamics*, Business Books Ltd, London.

Gillespie, T.D. (1978) 'Validation of the MVMA/HSRI Phase II straight truck directional response simulation', HSRI 4275, Highway Safety Research Institute, University of Michigan.

Hayes, G.G. (1980) 'Validation of truck handling simulation results, Vol. I, Summary Report', FHWA/RD-80/060, National Technical Information Service, Springfield, VA, 22161.

Huston, J.C. and Johnson, D.B. (1983) 'Basic analytical results for lateral stability of car/trailer systems', SAE Technical Paper 820136.

Klein, R.H. and Szostak, H.T. (1980) 'Development of maximum allowable hitch load boundaries for trailer towing', SAE Technical Paper 800157.

McHenry, B.G. and McHenry, R.R. (1988) 'HVOSM-87', SAE Technical Paper 880228.

McHenry, B.G. and McHenry, R.R. (1988) 'SMAC-87', SAE Technical Paper 880227.

Molnar, J. (date unknown) 'Automatic dynamic analysis of mechanical systems, ADAMS', Mechanical Dynamics Inc., Ann Arbor, Michigan.

Passarello, C.E. (1979) 'A simplified analysis of the steady-state turning of articulated vehicles', SAE Technical Paper 790185.

Reed, W.S. and Keskin, A.T. (1987) 'Vehicular response to emergency braking', SAE Technical Paper 870501.